Biophysical Chemistry, 38 (1990) 123–130
Elsevier

BIOCHE 01505

Conformational changes associated with the nicking and activation of botulinum neurotoxin type E

Bal Ram Singh and B.R. DasGupta

Food Research Institute, University of Wisconsin, 1925 Willow Drive, Madison, WI 53706, U.S.A.

Received 30 January 1990
Revised manuscript received 23 April 1990
Accepted 26 April 1990

Toxin activation; CD; Conformational analysis; Fluorescence quenching; Neurotoxin; Secondary structure; Tyrosine exposure; Tryptophan probing

Secondary and tertiary structural parameters of type E botulinum neurotoxin in the unactivated single-chain and activated two-chain (i.e., after proteolytic cleavage) forms were analyzed using circular dichroism, derivative absorption and fluorescence spectroscopy. The estimated secondary structures (22 and 20% α-helix, 44 and 44% β-pleated sheets, and 34 and 36% random coils for the single- and two-chain neurotoxins, respectively) indicated that virtually no change occurred upon nicking of the single-chain neurotoxin. About 57% of the 70 Tyr residues were exposed in the single-chain form, which increased to 62% in the two-chain form. Fluorescence quenching experiments with neutral, anionic and cationic quenchers indicated that about 40% of the maximum accessible fluorescent Trp residues were exposed on the surface of the single-chain neurotoxin as compared to only 20% in the case of the two-chain neurotoxin. Acrylamide was the most effective quencher with a fraction accessibility of 0.56 and 0.48 of maximum accessible Trp fluorescence residues in the single and two-chain forms of the neurotoxin, respectively. Native polyacrylamide gel electrophoresis of the two forms of the neurotoxin revealed greater mobility for the two chain form. This indicates that the surface charges in the single-chain neurotoxin were altered upon nicking. These observations suggest that nicking of the single-chain type E neurotoxin results in refolding and redistribution of the surface charges of the neurotoxin.

1. Introduction

Botulinum neurotoxins are a group of approx. 150 kDa proteins produced by *Clostridium botulinum* which are pharmacologically similar but serologically distinguishable. There are seven known serotypes (types A–G) of botulinum neurotoxins [1].

The neurotoxins, synthesized as a single-chain molecules, acquire higher toxicity (LD_{50}/mg protein) following posttranslational modification in bacterial culture [2], which involves nicking of the single-chain protein at one-third the distance from the NH_2-terminus. The resulting two-chain neurotoxin consists of light (L, ~ 50 kDa) and heavy (H, ~ 100 kDa) chains, that remain linked by a disulfide bridge and noncovalent interactions [3,4]. When nicking does not occur in bacterial cultures (e.g., in type E), it can be carried out in vitro by trypsin. Although controlled digestion of the single-chain type E neurotoxin with trypsin nicks the neurotoxin and increases its toxicity approx. 100-fold (activation), the kinetics of nicking and activation of type B neurotoxin are not the same [5]. This and other experiments [6] indicate that nicking is not the primary factor underlying activation. However, irrespective of the primary cause of activation, the molecular basis of the higher activity is likely to be the conformation of the two-chain form of the neurotoxin. It is not

Correspondence address: B.R. DasGupta, Food Research Institute, University of Wisconsin, 1925 Willow Drive, Madison, WI 53706, U.S.A.

known what conformational changes in the type E neurotoxin are induced by proteolytic processing and whether activation of the type E neurotoxin is due to such changes.

The well-known pharmacological action of botulinum neurotoxin is at the neuromuscular junctions. The neurotoxin binds exclusively to the presynaptic membrane, enters the nerve ending and causes an intracellular lesion(s); blockage of acetylcholine release causes flaccid muscle paralysis [7,8]. It is unclear whether the activation of type E neurotoxin, i.e., increase in lethality, is a manifestation of enhanced binding to the 'receptors' on the membrane, internalization or intracellular blockage, or an additive effect of enhanced activity due to more than one of these three steps.

We investigated the conformation of the type E neurotoxin before and after activation (treatment with trypsin) in terms of the secondary structures by means of circular dichroism, surface exposure of Tyr residues using second-derivative ultraviolet absorption spectroscopy and Trp accessibility employing the Trp fluorescence quenching techniques. Although no changes in secondary structures were evident, significant differences in the accessibility of Trp residues and in the surface exposure of Tyr residues were observed. In addition, electrophoresis under nondenaturing conditions suggested that change in the surface charges occurred upon nicking of single-chain type E neurotoxin.

2. Materials and methods

Single-chain type E neurotoxin, isolated from cultures of *C. botulinum* type E (strain Alaska E-43) according to Giménez and Sugiyama [9], was nicked as follows; neurotoxin and trypsin (Worthington), both dissolved in 10 mM sodium phosphate buffer (pH 6.0) and mixed in a 40 : 1 (w/w) ratio were incubated at room temperature (23–25 °C) for 90 min. The reaction was stopped by incubating the mixture with soybean trypsin inhibitor (STI) linked to agarose beads (Sigma, St. Louis, MO) for 30 min at room temperature. The nicked neurotoxin was recovered by filtering the mixture through a 0.2 μm Acrodisc filter (Gelman Sciences). Neurotoxin nonspecifically bound to the agarose beads was extracted with 0.6 M NaCl dissolved in 10 mM sodium phosphate buffer (pH 6.0). The filtered neurotoxin (before extraction with 0.6 M NaCl) was used directly for experiments following appropriate dilutions, while the 0.6 M NaCl-extracted neurotoxin was precipitated with ammonium sulfate (39 g/100 ml). The precipitated neurotoxin was redissolved in 10 mM sodium phosphate buffer (pH 6.0) and dialyzed against the same buffer before use. Each protein preparation was filtered through a 0.2 μm filter before optical measurements. Utrapure guanidine · HCl (Schwarz/Mann, Cleveland, OH) and other chemicals used were of the highest quality available commercially. All buffers and solutions were made up in deionized distilled water.

Absorption spectra were recorded on a Uvikon 860 (Kontron Instruments). CD spectra were recorded on a Jasco J-20 CD/ORD spectropolarimeter as described elsewhere [10]. Secondary structures were estimated according to Chang et al. [11] using the program provided by Drs J.T. Yang and C.-S.C. Wu of the University of California, San Francisco.

The degree of Tyr exposure, α, was estimated according to Ragone et al. [12].

$$\alpha = \frac{\gamma_n - \gamma_a}{\gamma_u - \gamma_a} \times 100 \qquad (1)$$

where γ_n and γ_u are the derivative peak ratios, a/b (see fig. 3 for notation), of the neurotoxins in the native (in 10 mM sodium phosphate buffer, pH 6.0) and unfolded (incubated in the pH 6.0 buffer containing 6 M guanidine · HCl for 30 min at 23 °C) states. γ_a is the derivative peak ratio of a mixture of free Tyr and Trp residues in the same molar ratio as the neurotoxin. The Tyr/Trp molar ratio was taken as 4.376 for the type E neurotoxin based on the published amino acid composition [4].

Trp fluorescence spectra of the neurotoxins were recorded on an SLM 8000 'smart' spectrofluorometer (SLM Instruments) at room temperature (23–25 °C). An excitation wavelength of 295 nm was used to excite preferentially Trp residues. The slit widths on both excitation and emission monochromators were set at 4 nm. Spectral resolution

for excitation and emission monochromators was fixed at 2 nm. To minimize the inner filter effect, fluorescence measurements were made with protein concentrations such that A_{295} was less than 0.1.

For Trp fluorescence quenching experiments, stock solutions of KI (5 M), CsCl (5 M) and acrylamide (8 M) were prepared. To 700 μl protein solution, 1–5 μl of a quencher was added in several steps (total of 19 μl) and the fluorescence at the emission maximum was recorded after each addition. Fluorescence intensities were corrected for the dilutions. In the case of acrylamide, the fluorescence intensity was also corrected for the absorbance due to acrylamide at the excitation wavelength (295 nm) according to the method of Eftink and Ghiron [13]. The quenching data were analyzed according to Stern-Volmer plots [13]:

$$\frac{F_0}{F} = 1 + K_{sv}[Q] \quad (2)$$

where F_0 and F represent the fluorescence intensities at the emission maxima in the absence and presence, respectively, of a given concentration, [Q], of quencher. K_{sv} is the Stern-Volmer quenching constant.

A modified Stern-Volmer analysis [15] was performed according to the equation

$$\frac{F_0}{\Delta F} = \frac{1}{f_a} + \frac{1}{f_a K_Q[Q]} \quad (3)$$

where F_0 and ΔF denote the steady-state fluorescence in the absence of any quencher and the difference in steady-state fluorescence in the presence of a given concentration of quencher, [Q]. K_Q is the effective quenching constant, and f_a denotes the fraction of maximum accessible fluorescence.

Native (nondenaturing conditions) and SDS-polyacrylamide gel electrophoresis were run on a Phast System (Pharmacia) electrophoretic unit using an 8–25% gradient and also 7.5% homogeneous gels (0.45 mm thick, in 0.112 M acetate–0.112 M Tris buffer, pH 6.4). The stacking gels were 4.5% acrylamide (A), 3% N,N'-methylenebisacrylamide (C) for the gradient gel and 5% A, 3% C for the homogeneous gel. Agarose (2%) buffer strips used for running electrophoresis were presoaked in 0.88 M L-analine, 0.25 M Tris buffer, pH 8.8. Electrophoresis was performed at 400 V for gradient gels and 600 V for the homogeneous gel for approx. 600 A V h according to the Phast System manual provided by Pharmacia.

The native (nonactivated) and trypsinized (activated) neurotoxins migrate on SDS-polyacrylamide gel electrophoresis under reducing conditions as single- and two-chain proteins, respectively, hence they are referred to as unnicked (or single-chain) and nicked (i.e., two-chain) proteins.

3. Results

3.1. Secondary structure

The CD spectra of the single- and two-chain neurotoxins (fig. 1) are virtually identical with the negative double CD maxima at approx. 221 and approx. 207 nm and the negative minima at 213 ± 1 nm. The mean residue weight ellipticities, θ_{MRW} were very similar in both forms. For example, at 207 ± 1 nm, the θ_{MRW} values were $-11\,243 \pm 58$ and $-11\,532 \pm 181$ degree cm^2 dmol^{-1} for the single- and two-chain neurotoxins, respectively. The apparent secondary structures derived from the CD spectra were 22 and 20% α-helix, 44 and 44% β-pleated sheets, no β-turns, and 34 and 36% random coils, respectively for the single and two-chain neurotoxins (table 1). Although the secondary structure estimation shows no β-turns, it is unlikely that such a large protein has no turns. The method of Chang et al. [11] is especially weak in the estimation of β-turns. The predicted CD spectra of the single- and two-chain type E neurotoxins are plotted along with the experimental spectra in fig. 1a and b, respectively. The predicted spectra are calculated from the estimated secondary structure contents according to the method of Chang et al. [11].

3.2. Tyr exposure

The degree of Tyr exposure on the surface of proteins was determined using second-derivative ultraviolet absorption spectroscopy. Fig. 2 shows

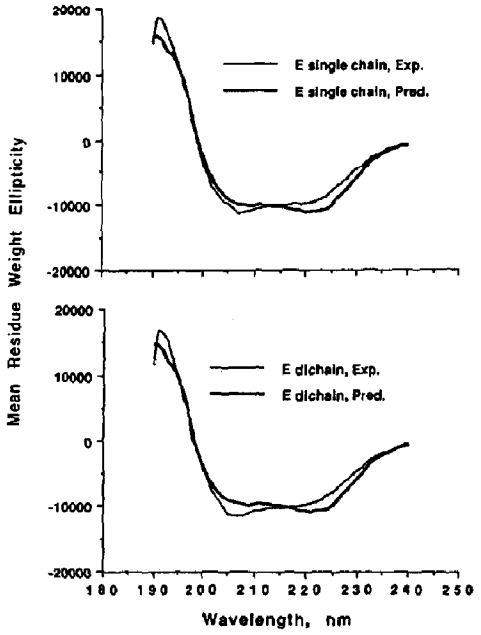

Fig. 1. Experimentally recorded (Exp.) and predicted (Pred.) CD spectra of single chain (upper panel) and two-chain (lower panel) type E neurotoxins. The CD spectra of 0.14–0.16 mg/ml neurotoxins, dissolved in 10 mM sodium phosphate (pH 6.0) were recorded at 23–25°C using a 1 mm path length quartz cuvette. The predicted spectra were obtained using the estimated values of α-helix, β-sheets and β-turns according to Chang et al. [11].

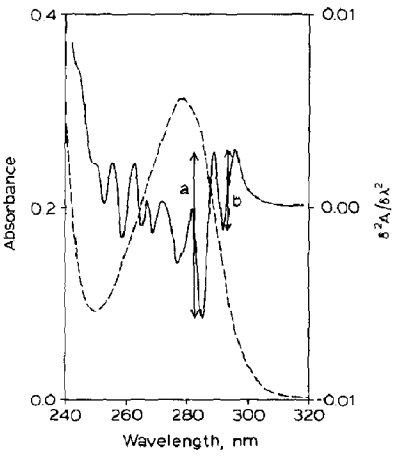

Fig. 2. Absorption (------) and second derivative (———) spectra of single-chain type E neurotoxin dissolved in 10 mM sodium phosphate (pH 6.0). The spectra were recorded at 23–25°C. The notation *a* represents the arithmetic sum of the $\delta^2A/\delta\lambda^2$ at 284.5 and 288.5 nm. The notation *b* represents the arithmetic sum of $\delta^2A/\delta\lambda^2$ at 291.5 and 295.5 nm.

the absorption and second-derivative spectra of the single-chain neurotoxin dissolved in 10 mM sodium phosphate buffer (pH 6.0). The derivative spectrum (between 280 and 300 nm) shows two negative peaks at 284.5 and 291.5 nm and two positive peaks at 288.5 and 295.5 nm. The ratio of *a* (arithmetic sum of the $\delta^2A/\delta\lambda^2$ at 284.5 and the $\delta^2A/\delta\lambda^2$ at 288.5 nm) and *b* (arithmetic sum of the $\delta^2A/\delta\lambda^2$ at 291.5 nm and the $\delta^2A/\delta\lambda^2$ at 295.5 nm) was 2.14 ± 0.04 (table 2). Upon denaturation with 6 M guanidine · HCl, $\delta^2A/\delta\lambda^2$ at 283.5 and 288.5 nm increased substantially (spectrum not shown) and the a/b ratio was 3.86 ± 0.14 (table 2). The second-derivative spectra of the two-chain neurotoxin show two positive peaks at 288.5 and 295.5 nm and two negative peaks at 285 and 291.5 nm (fig. 3), very similar to the single-chain neurotoxin (fig. 2). However, a minor difference was noted in the peak ratios of the positive peaks at 288.5 and 295.5 nm. The ratio was 1.04 and 0.87 for the single- and two-chain neurotoxins, respectively. The a/b ratio for the two-chain neurotoxin was 2.28 ± 0.24. Upon denaturation with 6 M guanidine · HCl, the intensities of the peaks at $\delta^2A/\delta\lambda^2$ at 283.5 and 287.0 nm increased (spectrum not shown). The a/b ratio increased to 3.79 ± 0.15 (table 2).

The degree of Tyr exposure was estimated to be 57.4 and 61.9% for single- and two-chain neurotoxins, respectively (table 2), which indicates small

Table 1

Secondary structure analysis of the single- and two-chain forms of type E botulinum neurotoxin, in 10 mM sodium phosphate buffer (pH 6.0) derived from far-ultraviolet CD spectra

The secondary structures were estimated using mean residue ellipticities between 240 and 190 nm at 1 nm intervals according to the method of Chang et al. [11].

Neurotoxin	α-Helix (%)	β-Pleated sheets (%)	β-Turns (%)	Random coils (%)
Single-chain	21.75 ± 1.06	44.00 ± 2.12	0.00	34.25 ± 1.06
Two-chain	19.75 ± 2.47	44.25 ± 1.77	0.00	36.00 ± 0.71

Table 2

The degree of Tyr exposure in the single- and two-chain forms of type E botulinum neurotoxin as determined by second derivative ultraviolet absorption spectroscopy

γ_n, a/b ratio of the native neurotoxin (see fig. 2 for the notation of a and b); γ_u, a/b ratio in the unfolded neurotoxin with 6 M guanidine·HCl; x, Tyr/Trp ratio; γ_a, a/b ratio of a mixture of free Tyr and Trp in the same ratio as in the neurotoxin, calculated using the equation:

$$\frac{A_x + B}{C_x + 1} \qquad (4)$$

where A, B and C are constants (taken from ref. 12) and x denotes the Tyr/Trp ratio. Numbers of replicate experiments are indicated in parentheses. Standard errors of means for single- and two-chain γ_n are ± 0.02 and ± 0.07, respectively.

Neurotoxin	γ_n	γ_u	x	γ_a	α (%)
Single-chain	2.14±0.05 (8)	3.86±0.14 (3)	4.376	−0.179	57.4
Two-chain	2.26±0.13 (4)	3.79±0.15 (2)	4.376	−0.179	61.9

alterations in the Tyr exposure of the single-chain neurotoxin upon nicking.

3.3. Trp topography

The topography of Trp residues was probed by the fluorescence quenching technique using anionic (I^-), cationic (Cs^+), and neutral (acrylamide) quenchers. The Trp fluorescence spectra of both the single- and two-chain forms showed emission maxima at 334 nm (spectra not shown). A Stern-Volmer analysis (plots not shown) of acrylamide quenching revealed Stern-Volmer quenching constants (K_{SV}) of 2.74 and 2.64 M^{-1} for the single- and two-chain neurotoxins, respectively (table 3).

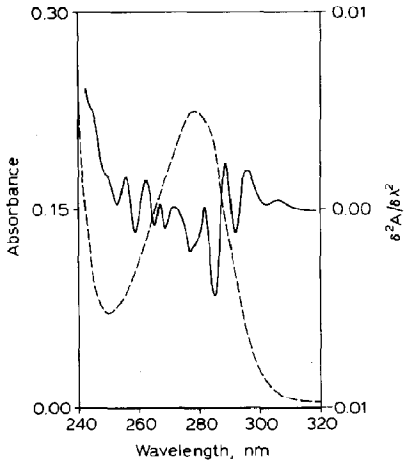

Fig. 3. Absorption (------) and second derivative (———) spectra of two-chain type E neurotoxin dissolved in 10 mM sodium phosphate (pH 6.0). Other details as in fig. 2.

The modified Stern-Volmer analysis for acrylamide quenching of Trp fluorescence revealed K_Q (effective quenching constant) and f_a (fraction of accessible fluorescence) of 7.62 M^{-1} and 0.56 for the single-chain neurotoxin and 8.83 M^{-1} and 0.48, for the two-chain neurotoxin, respectively (table 3).

The ionic quenchers (I^- and Cs^+), unlike the nonionic acrylamide, were substantially less effective quenchers. Stern-Volmer constants for I^- quenching were 1.26 and 0.8 M^{-1} for the single- and two-chain neurotoxin, respectively (table 3). The Stern-Volmer plots for I^- quenching are shown in fig. 4. Modified Stern-Volmer analysis revealed K_Q and f_a values of 16.05 M^{-1} and 0.25 for the single-chain neurotoxin and 8.82 M^{-1} and 0.19 for the two-chain form. The modified Stern-Volmer plots are shown in fig. 5. The cationic

Table 3

Trp fluorescence quenching parameters of the single- and two-chain forms of type E botulinum neurotoxin

Quenchers	Single-chain form			Two-chain form		
	K_{SV} (M^{-1})	K_Q (M^{-1})	f_a	K_{SV} (M^{-1})	K_Q (M^{-1})	f_a
I^-	1.26	16.05	0.25	0.80	8.82	0.19
Cs^+	0.58	6.29	0.16	– [a]	–	–
Acrylamide	2.74	7.62	0.56	2.64	8.83	0.48

[a] Fluorescence quenching was negligible.

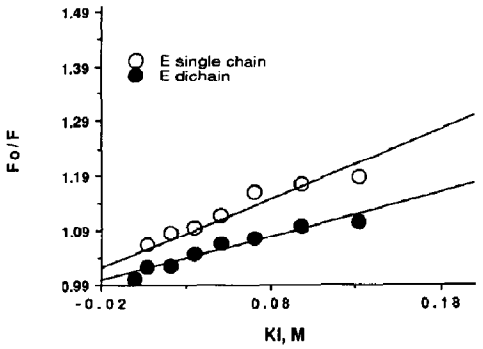

Fig. 4. Stern-Volmer plots for I^- quenching of Trp fluorescence in the single- and two-chain type E neurotoxins. F_0 and F represents the fluorescence intensities in the absence and presence of the indicated concentration of quencher (acrylamide), respectively. The excitation wavelength was 295 nm, and spectral resolution was fixed at 4 and 16 nm for excitation and emission monochromators, respectively.

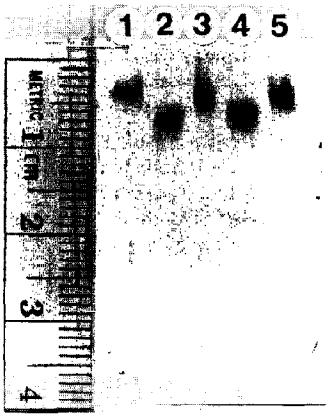

Fig. 6. Native polyacrylamide gradient (8–25%) gel electrophoresis of the single-chain (lanes 1, 3 and 5) and two-chain (lanes 2 and 4) type E neurotoxins. About 0.58 μg of single-chain neurotoxin and 0.79 μg of two-chain neurotoxin were applied in their respective lanes. The neurotoxin bands were stained with Coomassie brilliant blue.

quencher Cs^+ was the least effective for both forms of the neurotoxin; K_{SV} for the single-chain neurotoxin was 0.58 M^{-1} (table 3), and for the two-chain neurotoxin it was negligible. Because of the negligible quenching in the two-chain form, modified Stern-Volmer analysis of Cs^+ quenching was carried out for the neurotoxin only in the single-chain form. The derived values of K_Q and f_a for Cs^+ quenching were 6.29 M^{-1} and 0.16, respectively (table 3).

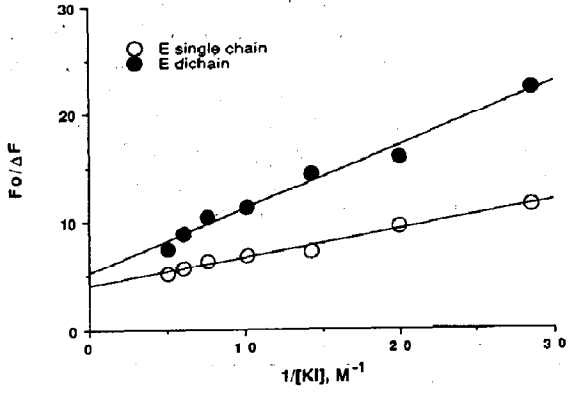

Fig. 5. Modified Stern-Volmer plots for I^- quenching of Trp fluorescence in the single- and two-chain type E neurotoxins. F_0, fluorescence intensity in the absence of any quencher; ΔF, difference in fluorescence intensities after adding a given concentration of quencher (acrylamide). Conditions for recording fluorescence spectra were the same as described in fig. 4.

3.4. Surface charges

Electrophoresis on a native polyacrylamide gel (fig. 6) showed a difference in the mobility between the trypsinized and native neurotoxin. Faster migration of the trypsinized neurotoxin towards the positive electrode indicated that the neurotoxin, following nicking, acquired more net negative charge. The neurotoxin in single- and two-chain forms, had identical electrophoretic mobility on SDS-polyacrylamide gel electrophoresis [9].

4. Discussion

The secondary structures of the neurotoxin undergo virtually no change upon nicking (table 1). This indicates that the neurotoxin retains the basic structural core of the protein likely to be essential for the toxic activity. This is consistent with our earlier finding that the three different serotypes (A, B and E) of the botulinum neurotoxins have basically the same pattern of secondary structures

[16] although they vary in toxicity approx. 1000-fold. Peptide cleavage by trypsinization may not influence the secondary structure, the core of the polypeptides' conformation, but could affect polypeptide folding (tertiary structure) which in turn may provide clues on the activation of the neurotoxin.

A significant change in polypeptide folding is likely to affect the degree of Tyr exposed to the protein surface. We observed only approx. 4% increase in Tyr exposure upon nicking of the single-chain type E neurotoxin (table 2). There are 70 Tyr residues in the type E neurotoxin. Thus, about 40 Tyr residues (57.4% of the 70) are exposed in the single-chain form whereas 43 Tyr residues (61.9% of the total of 70) are exposed in the two-chain neurotoxin. The degree of Tyr exposure calculated based on second-derivative ultraviolet spectroscopy qualitatively agrees with an earlier study [17], where the alkaline pH induced-difference spectra demonstrated that 45 Tyr residues in the single-chain neurotoxin could be ionized. However, all the Tyr residues in the two-chain neurotoxin were ionized by alkali. The molecular topography of the Tyr residues is apparently important for the toxicity of the type E neurotoxin, since the modification of 10–12 Tyr residues by tetranitromethane abolished the toxicity [18].

Trp fluorescence quenching is used to probe the microenvironments of Trp residues [19,20]. A change in fluorescence of one or more of the 16 Trp residues in type E neurotoxin [4] can, therefore, reflect change(s) in polypeptide folding. Among the three quencher probes used in this study, acrylamide was the most effective (table 3) at quenching the Trp fluorescence of both single- and two-chain neurotoxins. Acrylamide, a neutral molecule, can penetrate the protein matrix and is, therefore, used to investigate the accessibility of fluorescent Trp residues in hydrophobic domains [21]. The accessible fraction of fluorescent Trp residues in the single- and two-chain forms was 56 and 48%, respectively (table 3, f_a values). Thus, about half of the fluorescent Trp residues were not accessible even to acrylamide. Such low accessibility suggests that a significant fraction of the fluorescent Trp residues are buried deep within the polypeptide folds which hinders diffusion of the quencher.

Fluorescence quenching by all the three quenchers including ionic quenchers (I^- and Cs^+) appears to be collisional, since no upward curvature was observed in their Stern-Volmer plots [20]. This suggests the absence of static quenching which is relatively more strongly affected by charge, pH or ionic strength of the protein solution.

Trp fluorescence quenching experiments with I^- indicated that the fluorescent Trp residues were only slightly more accessible in the single-chain form than in the two-chain neurotoxin (cf. f_a values in table 3). However, I^- was considerably more effective in quenching the Trp fluorescence of the single-chain neurotoxin as compared to the two-chain form (as indicated by the K_{SV} and K_Q values; table 3). Lower f_a and K_{SV} values for I^- relative to acrylamide are consistent with the conclusion that most of the fluorescent residues are buried in the protein matrix of the neurotoxin (vide supra). Comparison of the quenching parameters for I^- and acrylamide is reasonable, since both have a quenching efficiency of unity [20]. In such a case, the difference in K_{SV} and K_Q values would reflect the difference in the microenvironments of the fluorescent Trp residues.

The cationic quencher, Cs^+, was the least effective in quenching Trp fluorescence in the type E neurotoxin. Only 16% of the fluorescent Trp residues were accessible to Cs^+ in the single-chain type E neurotoxin while no quenching was observed in the two-chain form (table 3). The f_a values for I^- and Cs^+ quenching are mutually exclusive, hence their sum represents the fraction of fluorescent Trp residues on the surface of the protein which are accessible to the two ionic quenchers. Thus, about 41% (sum of 0.25 and 0.16) of the fluorescent Trp residues are apparently on the surface of the single-chain neurotoxin and 19% (sum of 0.19 and zero) on the surface of the trypsinized neurotoxin. Since 48–56% of the fluorescent Trp residues in the single- and two-chain forms of the neurotoxin are accessible to acrylamide, it appears that additional Trp residues not accessible to the ionic probes are accessible to the neutral probe acrylamide.

This study indicates that while virtually no alteration in the secondary structure of type E neurotoxin occurred upon nicking (i.e., during activation), significant change in the tertiary structure was observed on monitoring the microenvironment of Trp residues. Change in the tertiary structure included only a small difference in the degree of Tyr exposure. It is possible that the changes take place in small segments of the polypeptide which affect the Trp but not the Tyr residues. The exposure of Tyr residues is derived from the absorption characteristics of the chromophores which is not as sensitive a technique as the method based on the fluorescence properties. Furthermore, the degree of Tyr exposure indicates an average of the exposed Tyr residues, therefore on average, the degree of Tyr exposure may not show any substantial difference even after a significant change in protein folding. This is more likely with proteins such as the neurotoxin which has a large number of Tyr residues. A refolding of the polypeptide structure could result in the redistribution of charges as indicated by the difference in electrophoretic mobility of the single- and two-chain neurotoxins. The two-chain neurotoxin acquires an additional anionic charge due to the formation of a new C-terminus of the light chain, i.e., a COO^- group. This additional anionic site could partly contribute to the greater electrophoretic mobility of the two-chain neurotoxin towards the anode (fig. 6). However, the data on Trp fluorescence in the case of ionic solute molecules (table 3) suggest an alteration of charge distribution in the vicinity of the Trp residues, implying that the difference in electrophoretic mobility may not be entirely explained by peptide cleavage during nicking.

Yokosawa et al. [22] obtained nonidentical peptide maps of the chymotryptic digests of the type E neurotoxin before and after activation. The differences in chymotrypsin-susceptible sites between the two forms of the neurotoxins were ascribed to conformational differences, consistent with the data presented in this report.

Acknowledgements

This study was supported in part by NIH grants NS 17742 and NS 24545, Department of Defence-University Research Instrumentation Program Awards DAAG 29-83-G-0063 and DAAL 03-87-G-0089, the Food Research Institute and the College of Agricultural and Life Sciences of the University of Wisconsin-Madison.

References

1 C.L. Hatheway, in: Botulinum neurotoxin and tetanus toxin, ed. L.L. Simpson (Academic Press, San Diego, 1989) p. 3.
2 G. Sakaguchi, Pharmacol. Ther. 19 (1983) 165.
3 B.R. DasGupta, in: Biomedical aspects of botulism, ed. G.E. Lewis, Jr (Academic Press, New York, 1981) p. 1.
4 V. Sathyamoorthy and B.R. DasGupta, J. Biol. Chem. 260 (1985) 10461.
5 I. Ohishi and G. Sakaguchi, Infect. Immun. 17 (1977) 402.
6 B.R. DasGupta and H. Sugiyama, Infect. Immun. 6 (1972) 587.
7 L.L. Simpson, Pharmacol. Rev. 33 (1981) 155.
8 L.L. Simpson, Annu. Rev. Pharmacol. Toxicol. 26 (1986) 427.
9 J.A. Gimenez and H. Sugiyama, Appl. Environ. Microbiol. 53 (1987) 2827.
10 B.R. Singh and B.R. DasGupta, Mol. Cell. Biochem. 85 (1989) 67.
11 T.C. Chang, C.-S.C. Wu and J.T. Yang, Anal. Biochem. 91 (1978) 13.
12 R. Ragone, G. Colonna, C. Balestrieri, L. Servillo and G. Irace, Biochemistry 23 (1984) 1871.
13 M.R. Eftink and C.A. Ghiron, J. Phys. Chem. 80 (1976) 486.
14 O. Stern and M. Volmer, Phys. Z. 20 (1919) 183.
15 S.S. Lehrer, Biochemistry 10 (1971) 3254.
16 B.R. Singh and B.R. DasGupta, Mol. Cell. Biochem. 86 (1989) 87.
17 A. Datta and B.R. DasGupta, Mol. Cell. Biochem. 81 (1988) 187.
18 M.A. Woody and B.R. DasGupta, Mol. Cell. Biochem. 85 (1989) 159.
19 J.R. Lakowicz, Principles of fluorescence spectroscopy (Plenum, New York, 1983).
20 M.R. Eftink and C.A. Ghiron, Anal. Biochem. 114 (1981) 199.
21 M.R. Eftink and C.A. Ghiron, Biochemistry 23 (1984) 3891.
22 N. Yokosawa, K. Tsuzuki, B. Syuto and K. Oguma, J. Gen Microbiol. 132 (1986) 1981.